Inertial Fusion : A Contribution of Accelerator Technology to the Energy Problem ?

Carlo Rubbia
CERN
CH - 1211 Geneva 23

1. INTRODUCTION.

High power Lasers have been so far the almost unique tool for bringing matter to high temperatures (>100 eV) and densities (>500x the solid density). A remarkable amount of work has been carried out which has permitted to highlight an exceedingly exciting field of physics and rich of applications. Most important, but not the only ones, are the contributions to the energy problem with Inertially Confined Fusion (ICF).

I would like to take this opportunity to elaborate on the possible contributions of specialized particle accelerators in order to bring matter to such extreme conditions. The idea of heating-up matter with heavy ions is not new. In recent years tremendous advances in particle accelerator techniques have made possible the realization of beam-beam colliders of extraordinary performances. As a result there is a vast fall-out of developments and ideas which could permit important progress in many other fields, including the one of ICF.

With the help of dedicated machines, heating matter with beams, a great inconvenience for conventional particle accelerators, can be an extremely powerful research tool. In particular heavy ions of sufficient energy — because of their high specific ionization, proportional to Z^2 — can produce extremely hot matter in the 200+500 eV temperature range. The first pioneering tests are now possible with the ion accelerator SIS/ESR in Darmstadt.

Matter at high temperature and density becomes radiation dominated. For instance inside a Stefan-Boltzmann black body radiator at a temperature 500 eV there is a X-ray flux of 10^{16} watts/cm^2. This radiation exerts an ablative pressure $>10^8$ bars and it provides a powerful tool for instance in order to ensure the implosion of small ICF pellets.

In my presentation I shall try to look at the future and delineate a number of conceptual progresses which could further extend the already important possibilities of the SIS/ESR programme, one step closer to the ultimate goals of practical applications, for instance in the field of energy production.

2. PARTICLE BEAMS FOR ENERGY PRODUCTION ?

Under the demands of fundamental research, the accelerator community has responded with a number of impressive fundamental developments. New types of accelerators and colliders have permitted a tremendous progress in the understanding of subnuclear physics. It is very likely that such a progress may lead also to practical applications in a number of other fields and in particular in that of energy production.

One of the most attractive forms of energy production is based on fusion, namely on some nuclear reactions in which light nuclei coalesce into larger nuclei with energy release. Although there are many possible fusion reactions, the need to overcome the Coulomb barrier makes the lowest Z reactions most attractive. Amongst them the best is the classic D–T process:

$$D + T \Rightarrow \alpha + n + 17.6 \text{ MeV} \qquad \{1\}$$

The specific energy release is $q_{DT} = 3.37\ 10^{11}$ J/gr. Whilst Deuterium is easily available for instance from the isotopic separation of water, Tritium is unstable and it must be produced. This in turn is best done by using natural Lithium (7.4 % ^{7}Li and 92.6 % ^{6}Li). Reactions $^7Li + n \Rightarrow T + \alpha + n$ and $^6Li + n \Rightarrow T + \alpha$ are induced by the neutron emitted in reaction {1}. The first reaction is endothermic and dominates for high-energy neutrons, while the reaction on ^{6}Li is a capture reaction and may make use of secondary neutrons from ^{7}Li. The combination of these two reactions can ensure a full breeding of the fuel, the excess yield helping to compensate for the inevitable losses due to geometry and absorptions. The net outcome is energy production by "burning" Deuterium and Lithium with Tritium as an intermediary.

Neutron-less reactions are of great interest since safety problems are considerably reduced. The most promising of such reactions appears to be that involving protons and Boron [1], both abundantly available, $^{11}B + p \Rightarrow 3\,\alpha + 8.7$ MeV which has a higher "burning point" than the classic D–T process but which does not directly emit secondaries outside the pellet. No Lithium blanket is needed and cooling can be performed with water. Radiation hazards and the inventory of radioactive substances are virtually suppressed. Some radiation is anticipated from secondary processes (see Table 1) but it is many orders of magnitude lower than that from an ordinary fission reactor.

Table 1. Secondary radiation emission from p-B^{11} reactor [1]

Reaction	Q (MeV)	Rate relative to $p+B^{11} \rightarrow 3\alpha$	Inventory for 1 GW (th.) plant (Curies)
$p + {}^{11}B \rightarrow {}^{12}C + \gamma$	16.0	5×10^{-5}	200 (1)
$p + {}^{11}B \rightarrow n + {}^{11}C$	- 2.8	1.5×10^{-5}	4×10^5 (2)
$\alpha + {}^{11}B \rightarrow n + {}^{14}N$	0.2	$\leq 10^{-3}$	$\leq 3 \times 10^5$(3)
$\alpha + {}^{11}B \rightarrow p + {}^{14}C$	0.8	$\leq 10^{-4}$	$\leq 10^3$ (4)
D-T Fusion Reactor	–	–	$\sim 10^8 - 10^9$

(1) O^{15} from activation of water shielding $\{t_{1/2}(O^{15}) = 2$ min$\}$.
(2) Thermal neutrons; $t_{1/2}\ (C^{11}) = 20$ min.
(3) Non-thermal neutrons; $1 \leq (E_n, E_p) \leq 4$ MeV.
(4) Annual production of ^{14}C; $t_{1/2}(^{14}C) \approx 6000$ y.

Finally hybrid schemes may be envisaged with an initial D-T ignition followed by B-p burning.

Natural boron is composed of 80.22% of ^{11}B and 19.78% of ^{10}B. Isotopically pure ^{11}B is desirable because in natural Boron ^{7}Be is produced by the reaction $^{10}B + p \Rightarrow {}^{7}Be + \alpha +$ 1.148 MeV. ^{7}Be is β–unstable with $\tau_{1/2} \approx 53$ days and it decays into stable ^{7}Li with a 487 keV γ-ray. Economical, large scale isotope separation by fractional distillation of BF_3 is a well-established technology. Boron-hydrogen compounds of the type B_5H_9 are stable liquids.

If possible on a practical scale, fusion energy will be

(1) *Inexhaustible* : for instance 28 million of barrels of oil, the daily world' s consumption is equivalent to 170 kg of Deuterium and 500 kg of Lithium.

(2) *Ecologically clean* : this applies especially to the ^{11}B-p reaction. In the case of the D-T reaction neutrons are abundantly produced and there is a considerable stock-pile of Tritium, however in controllable conditions.

(3) *No major impact on the environment* : it avoids the main concern about fossils burning namely the emission of large quantities of "green house" gases.

Particle accelerators appear as the most promising drivers for a power reactor based on ICF. In particular, accelerators are unique in having a high driver efficiency ($\geq$ 25%), a high repetition rate ($\geq$ 25 Hz) and a high durability. Accelerator technology is highly developed and extremely reliable. These are crucial points for an industrial power reactor. In contrast LASERS are excellent devices for research and development in order to demonstrate the basic underlying phenomenology.

3. THE PRINCIPLES OF ICF.

3.1. General considerations. ICF [2] draws its inspiration from the idea of producing many small explosions in close succession in order to realize a "combustion engine". Targets are small capsules containing the fuel: ignition and burning are achieved at its centre with imploded and highly compressed fuel. The D-T reaction is the easiest. Because of its small dimensions the capsule is transparent to neutrons and the Tritium breeder must be located outside, in the heat-absorbing blanket. The shortcoming is a strong neutron flux in the combustion chamber. Second generation devices should make use of the more advanced reaction ^{11}B-p and there is hope that the difficulty mentioned above is only temporary.

The reaction is self-sustained when the so-called Lawson criterion [3] is satisfied: the specific fusion energy output $17.6\ n^2 \langle\sigma v\rangle\ t_c$ MeV must be equal or larger than the energy spent to heat up the fuel $\approx 6\ n\ k_BT$, where n is the density of Deuterium ions per unit of volume, $\langle\sigma v\rangle$ is the Maxwell-Boltzmann averaged value of the product $v\sigma$, where v is the speed of the ions and σ the cross section, t_c is the confinement time and k_BT is the temperature expressed in terms of energy. The actual value of $\langle\sigma v\rangle$ for a number of reactions is shown in Fig. 1. A more practical criterion is obtained by requiring 30% fuel burn, which for D-T and temperatures of the order of $k_BT \approx 20$ keV implies $n\ t_c \geq 10^{21}\ m^{-3}\ s$. In the case of the neutron-free reaction $p-{}^{11}B$ comparable values of $\langle\sigma v\rangle$ are expected, but with higher $k_BT \approx 50$–100 keV.

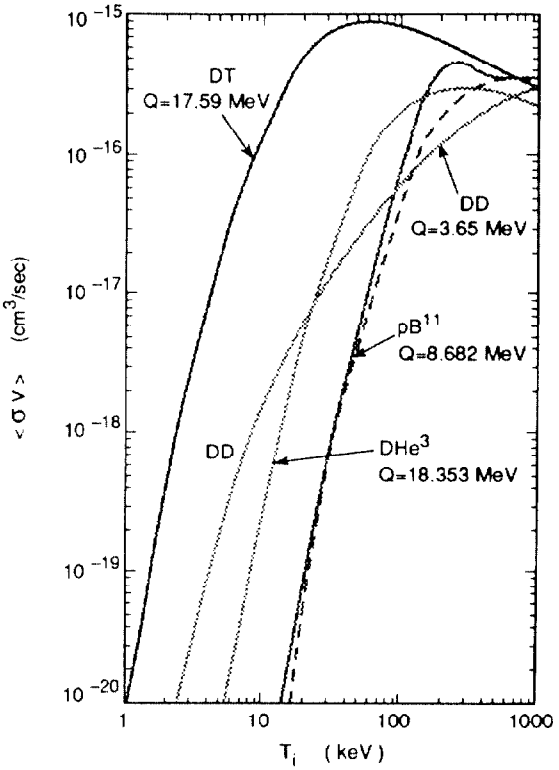

Fig. 1. *Temperature dependence of main fusion reactions.*

Both ICF and Magnetically Confined Fusion (MCF) must satisfy Lawson's criterion, but with a very different choice of parameters:

Confinement	n(m-3)	t_c (sec)	$n\ t_c$
Magnetic	10^{20}	10	10^{21}
Inertial	10^{31}	10^{-10}	10^{21}

In the case of ICF there is no appreciable confinement force and the confinement time is close to the disassembly time $t_c \approx \tau = R/c_s$, where c_s is the "sound" speed in the medium. Instead of $n\ t_c$ it is preferable to use the parameter ρR where ρ is the density and R is the radius of the sphere. The fraction ϕ of the fuel burnt during the period τ is then :

$$\phi = \frac{\rho\ R}{(H_B + \rho\ R)}\ ;\ H_B = 4\ c_s \frac{(m_D+m_T)}{\langle \sigma\ v \rangle}$$

H_B is the so-called "burn parameter" which for D-T and $k_BT \approx$ 20–50 keV is $H_B \approx 7.0$ gr cm^{-2}. The initial density, in order to satisfy the Lawson criterion, is a fast varying function of the fuel mass, $m_0 = 4/3\ \pi\ \rho\ R^3$. In order to burn for instance $\phi = 0.30$ of 1 mgram of D-T fuel ρ must be as high as 350 gr cm^{-3}, or equivalently 1750 times the liquid density. These requirements quickly relax with the size of the burning pellet. For instance a $\phi = 0.30$ burning condition for 10(30) mgram fuel requires a ρ about 550 (350) times the liquid density. Experiments with LASER compression have reached

densities in excess of 600 times the solid phase [4]. Clearly the Lawson criterion would suggest a relatively large inertially compressed mass so as to increase the burn-up due to the more extended disassembly time. Considerations on the survival of the combustion chamber would tend to limit the amount of exploding fuel at each shot and a compromise must be found between these two conflicting requirements.

Since both high temperature and density are needed, the driver's energy must be first converted into the kinetic energy of an imploding shell. Such energy should raise the temperature of the compressed fuel only after the required density is achieved. Therefore the specific energy yield, $q_{DT} = 3.37\ 10^{11}$ J/gr must largely exceed the energy required to bring the fuel to the ignition temperature $k_B T \geq 5$ keV, $\varepsilon_s = 4 \times 3/2 \times k_B T / (m_D + m_T) \approx 600$ MJ/gr. The factor $\phi q_{DT}/\varepsilon_s = 500\,\phi \approx 150$ is a gross over-estimate of the real gain because of the inefficiencies of the process. It is therefore preferable to ignite first a small portion of the fuel (the "spark region") and then let the spark propagate to the full fuel reservoir. This is described as the "central ignition and propagating burn" scenario and it is believed to be a necessary step for ICF. While the spark is done best with D-T, different fuels could be used for the main burning.

In order to secure continuing "burning", the thermo-nuclear energy deposited in the plasma by the nuclear reaction must exceed the energy losses due to radiation, hydrodynamical expansion etc. The burning plasma in MCF is optically thin for bremsstrahlung of electrons, which is the dominant mechanism of energy loss. While for D-T and sufficient temperatures the energy output is higher than these energy losses, in the case of the neutron-free reaction p-^{11}B the contrary is true (it will not "burn" !).

The situation is much more favourable in the case of ICF. There are two main reasons for this:

(1) The combustion rate is determined by the ion temperature T_{ion} and bremsstrahlung is a function of the electron temperature T_e. Since the energy of the combustion is slowly transferred from ions to electrons by Coulomb friction, T_e depends on the electron-ion coupling time, about four times larger in a low-density MCF plasma when compared to ICF. Consequently the ICF plasma stabilizes at a smaller T_e and has lower radiation losses, thus permitting the combustion to be better sustained.

(2) The pellet is optically thick. For an opacity length λ_a the pellet has $\lambda_a \rho R$ thickness units from the centre to the edge. Since $\rho R \approx H_B \approx 7.0$ gr cm^{-2}, the pellet fuel remains several units thick[1], even for the most transparent spectral components of the radiation. Most of the radiated energy is trapped inside the pellet and it actually helps uniformizing burning conditions.

Therefore in contrast with MCF, ICF allows second generation devices based on the p + ^{11}B reaction to be envisaged, which are far more acceptable in view of the reduced risks on the environment.

[1]The opacity is very high for low energy X-rays and stabilizes to about $\lambda_a \approx 2.0$ cm^2/g for ≥100 keV and high temperatures

3.2. Modelling. Computer simulations can be used to describe the implosion mechanism of pellets. The simplest calculations are performed in one dimension [5], namely the only spatial coordinate is the radius. In these calculations most of the instabilities are not appropriately described because spherical symmetry is assumed throughout. They are however quite useful to understand the basic features of the phenomenon. In Fig. 2a we display calculated [6] implosion movements.

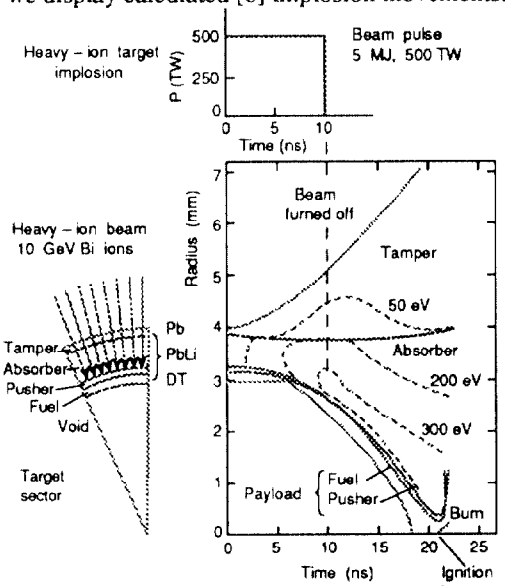

Fig. 2a. *Computer simulation of a pellet implosion [6].*

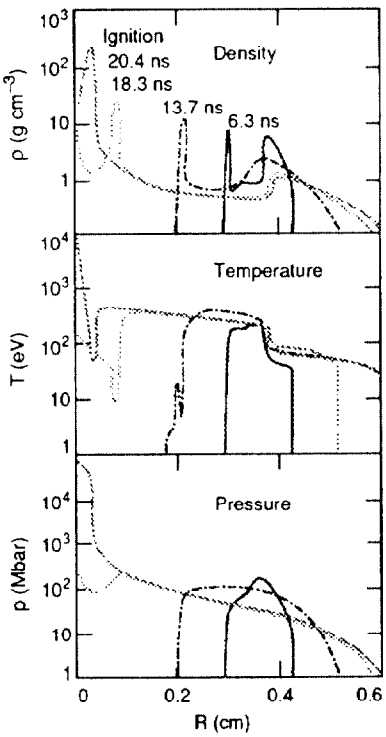

Fig. 2b. *Evolution of density, pressure and temperature in a pellet implosion according to computer simulations [6].*

In Fig. 2b one can clearly see how the spark formation proceeds with a rapidly rising pressure and temperature in the central region. As soon as central combustion starts, α-parti-

cles are heating the fuel propagating the burning throughout the whole sphere. The burn-up is extremely fast and the whole process is over in some tenths of a nanosecond.

A simple analytical model has been introduced by Meyer-ter-Vehn [7] and it can be used to get some insight of the process. In such a model it is assumed that while pressure is maintained constant throughout the sphere, there are two distinct regions, an inner one (ρ_S, T_S) in which the spark will occur where the temperature is high and an external colder region (ρ_C, T_C) of higher density extending to a radius R_f.

The two regions are sharply separated at the radius R_S. Two other relevant parameters characterizing the model are the so-called *isentrope parameter* $\alpha \geq 1$ which measures the preheat entropy and more generally the ability of transforming the motion into heat and the *hydrodynamic efficiency* η transforming the energy of the beams into kinetic motion $\eta_F = E_F/E_{beams}$. The inner region is described as an ideal hydrogen plasma and the outer, colder and higher density region as a degenerate electron gas. The gain $G = E_{TN}/E_{beams}$ is the ratio between the delivered thermo-nuclear energy E_{TN} and the energy delivered by the beams E_{beams}.

In the model one has to set somewhat arbitrarily the spark radius R_S as well as α and η. Typical parameters are $R_S \approx$ 75 μm and α = 1–3 and $\eta \approx$ 0.05–0.15. With these values, calculations compare well (see Fig. 3) with more sophisticated computer simulations (LLL).

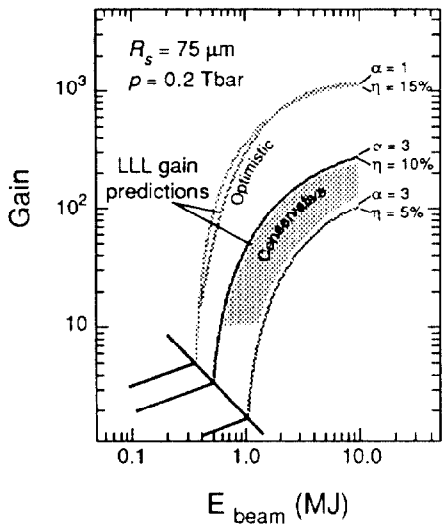

Fig. 3. *Calculated target gains from Ref. [7].*

3.3. Hydrodynamic instabilities. The one-dimensional calculations however ignore several critical issues in the target implosion and in particular instabilities due to hydrodynamic phenomena and driven by lack of perfect symmetry of the implosion geometry and of the beam depositions.

ICF target implosions are hydrodynamically unstable [8], due to the so-called Rayleigh-Taylor [9] instability (RTI) which is expected to occur wherever two liquids of different densities are strongly accelerated. This instability may cause density perturbations at the interface between the two liquids to grow in amplitude until there is a large scale mixing and interpenetration. Such a mixing and break-up would destroy the symmetry of compression and thus prevent high densities. In order to make the burning occur it is necessary to keep the growth rate of such phenomena sufficiently small over the relatively short implosion time (10–20 ns). In turn this means that the asymmetries in the initial conditions and the inhomogeneities must be as small as possible.

The instability in a uniformly accelerated fluid in the *linear theory* has been discussed by Chandrasekhar [10]. If the density ratio is large at the interface, the perturbation amplitude will grow exponentially with time $A(t) = A_0 e^{nt}$ with $n = \sqrt{2 \pi a/\lambda}$, where a is the acceleration and λ the wavelength of the perturbation. For the most dangerous modes in which $\lambda \approx d$, the thickness of the pusher may have $a = 2\times10^{15}$ cm s^{-2}, $d \approx (5.0–1.0)\times10^{-3}$ cm from which we find nt = 8–10, which imposes very strong requirements on the shell and heating non-uniformities [6].

Fortunately as soon as the scale of the perturbations becomes comparable to d, a *non-linear* regime sets in, which corresponds to the less destructive linear rather than exponential growth [11]. There is expectation for a limiting bubble motion speed given by $v_\infty = \sqrt{a \lambda/6 \pi}$. For $a = 10^{15}$ cm s^{-2}, $\lambda \approx 10^{-3}$ cm we find $v_\infty \approx 10^6$ cm s^{-1} to be compared with the implosion speed $v_{impl} = 3\times10^7$ cm s^{-1}. Therefore one might expect $v_\infty/v_{impl} \leq 1/30$ which will keep the phenomenon localized. Laser beam experiments [12] have shown a reduction in the growth rate with respect to the linear theory by a factor 1.5. Larger factors are however needed in order to secure a safe implosion of the pellet [13].

In order to study the effects of driving non-uniformities and in the absence of reliable experimental data, simulations are performed in two dimensions (R ; ϕ) [14].

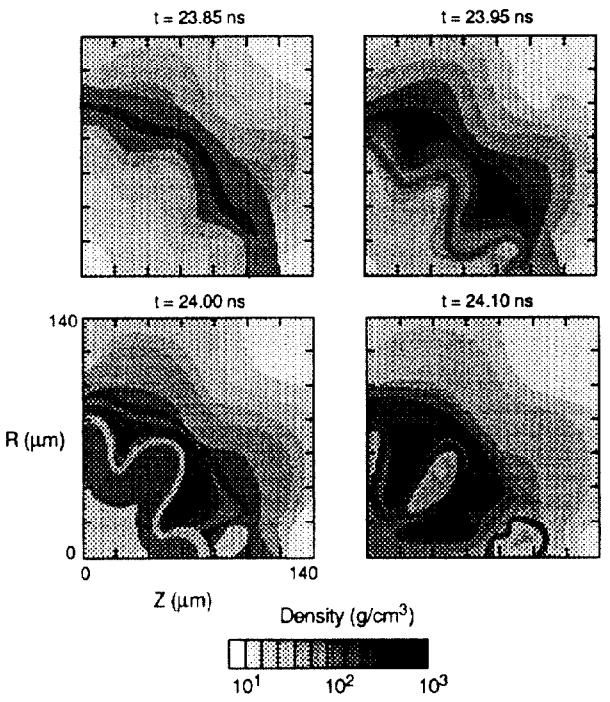

Fig. 4. *Computer simulation of RTI instabilities in the final compression phase due to driver non-uniformities [14].*

There are two critical areas in which disruptive effects due to the RTI may occur, i.e. (1) in the initial phase, when beam heated material outside accelerates dense material inwards and (2) in the final deceleration phase, when imploding pusher material falls into the stagnating compressed central fuel.

The effects of these instabilities simulated on a computer are rather spectacular (Fig. 4). This instability causes density perturbations with mixing and break-up which could destroy the symmetry of the compression process and eventually prevent high densities to occur.

It should be pointed out that there are important effects due to radiative transport which can strongly damp instabilities of hydrodynamical origin. In a nutshell, while in the radiative regime ($\rho c_s^3 << \sigma T^4$ — σ is the Stefan constant — i.e. the radiation energy is dominant over the kinetic energy) spikes tend to be smoothed out. The contrary occurs in the hydrodynamic regime ($\rho c_s^3 >> \sigma T^4$).

One can use computer simulations [14] to estimate the extent of permissible non-uniformities which still maintain the burning-up of the fuel. In Fig. 5 the ratio between the delivered energy E_{TN} is calculated with the one-dimensional approximation (in which RTI are absent) and a two-dimensional simulation with RTI instabilities. The non-uniformities are expressed in terms of the peak amplitude deviations $\Delta p/p$ of the deviations from symmetry expanded in its Legendre modes. Already a few percent non-uniformities are degrading the yield. This is more critical for the "near ignition" case: over-driving the pellet reduces the requirements on uniformity.

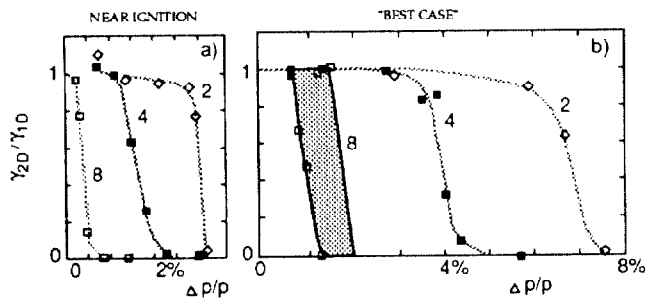

Fig. 5. *Yield reductions due to RTI. The abscissa Δp/p is the peak amplitude deviation from symmetry in the chosen Legendre mode [14].*

These studies have built up the belief that RTI is manageable provided extremely tight conditions are set on the symmetry of the drive, at the level of a few percent in the peak-to-valley amplitude. If these conditions are met the 1-D calculations are believed to be a valid approximation for the estimates of the gain.

3.4. Optimum pellet design for heavy ions. It has been already indicated that larger pellets operate with a longer rarefaction time $t_c \approx \tau = R/c_s$ and therefore smaller critical densities. While LASER driven pellets which have to operate with relatively low energy and high power are relatively tiny, ion beams can easily maintain power for a longer time, thus increasing the driving energy and the corresponding pellet size. With larger pellets rather remarkable performances can be met, as is given in a paper by Basko [15]. The pellet is relatively large (1 cm in diameter) and it is imploded by a supposingly fully symmetric 10 GeV Bi ion beam irradiation with a peak power of 720 TW during some 15 ns. As much as 61% of the 12 mgram of D-T fuel is burnt, leading to a gain in excess of 400 and an energy output of 2500 MJoules !

For an optimum mass of the pusher, 10–20 mgrams of fuel can be ignited by the 10 GeV Bi ion beam. These considerations suggest even larger pellets. Larger explosions may require a revision of some of the basic concepts in the design of the combustion chamber.

4. RADIATION DRIVEN "INDIRECT" DRIVE.

4.1. General considerations. Although many different methods have been considered, compression of the pellet needs an extremely uniform drive. The smallest lack of symmetrization is a source of instabilities of hydrodynamical nature before ignition (RTI) at the interface between pusher and fuel, especially just before ignition. As already pointed out, in order to be successful, the pellet implosion must proceed almost exactly symmetrically. A few percent deviations may be sufficient to hinder a successful burn-up. While the symmetrization of the very many beams needed to implode the pellet in the direct mode must be adjusted carefully at every shot, in the so-called "indirect drive" (ID) one makes use of an intermediary, smoothing step between the beam driver and the pellet, i.e. inserting the pellet inside a black-body *hohl-raum* cavity heated at some 300–400 eV. The flux of radiation inside an ideal black body is symmetric and independent of the shape of the volume. Symmetrization in ID relies primarily on a physical property of a black body, rather than on the matching accuracy between beams.

The beam energy is converted into soft X-rays which, after multiple reflections inside the cavity, exert pressure onto the pellet. The pressure is exerted by the ablation of the walls of the "pusher" under the effects of radiation. ID however is more complicated and less efficient when compared to the direct drive (DD) in which the compression is realized by a direct ablation of the capsule walls by the beam.

The outer walls of the cavity must be black and re-emit the radiation. High Z materials are to a good approximation "black" since for instance the mean free path for a 1 keV photon in Pb is 2 $\mu g/cm^2$. The cavity must have a good re-emission coefficient in order to ensure that the circulating flux is considerably larger than the source flux and it is symmetrizing the radiation on the capsule. It appears that a high re-emission coefficient requires the highest Z. Some 10 + 20 reflections are then be expected in an empty *hohl-raum*. On the other hand the walls of the capsule should be made of low Z with high absorbing power. Finally a critical parameter is the ratio A between the areas of the cavity and of the pellet. While large values of A ensure the best illumination uniformity, the transfer efficiency is best for small A values. A compromise value could be found for $A \approx 4$–6.

X-ray conversion can be realized with a variety of geometries. A single radiator is to be excluded since it is hard to

achieve the required uniformity and several "filamentary" radiators must be used. This geometry requires small beam spots and is adapted to high-energy beams. Another geometry consists in stopping the beams directly in the walls of the *hohlraum*. This is best suited to relatively low-energy beams because of the larger spot size and the shallow depth to absorb the beam. More complex geometries with diffusive materials inside the *hohl-raum* can also be considered.

4.2. Filamentary radiators. The radiator consists of a tiny cylinder of matter in which the ion beam is absorbed. This converter geometry can give a high conversion efficiency provided the deposited power densities are in excess of 10^{16} W/g. Light Z-radiators may show a fast efficiency drop-off at high power densities because the radiator becomes transparent at higher temperatures and can no longer dissipate radiatively the deposited power. The difference in efficiencies between medium and high Z is somewhat attenuated by the fact that the range of heavy ions f.i. in Au is about twice as long (in gr/cm^2) as that in Al.

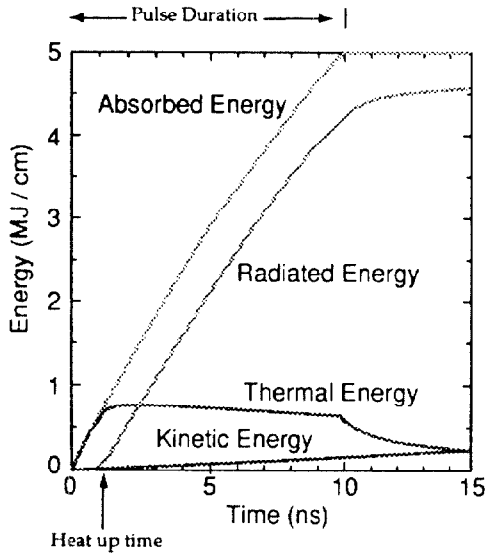

Fig. 6. *Time behaviour of a 1.5 mm radius filamentary radiator hit by an intense 5 MJ-pulse of Bi ion beam.*

It should also be noted that while the radiator warms up, the range shortens significantly. The time evolution of the phenomenon goes through three phases: (1) the heating phase during which the major fraction of the beam energy is used to provide the internal energy associated to the temperature; (2) the "quasi-steady" radiation emission with a high conversion efficiency; (3) the final disassembly of the radiator. The typical behaviour of a thin rod of material of 1.5 mm radius exposed to a 5 MJ-10 ns pulse of Bismuth ions with T = 10 GeV is shown in Fig. 6. About 90% of the beam energy is converted into soft X-rays.

The number and locations of filamentary radiators should be chosen in order to ensure the appropriate uniformity of illumination. Realistic calculations show that the two radiator geometry introduces residual asymmetries which are by no means negligible. A six- or eight-radiator configuration on the other hand looks much better and is preferable. With such a geometry a very uniform illumination can be achieved [16].

4.3. Diffuse radiators. A practical device based on several tiny filamentary radiators present severe alignment problems. The hohlraum could be instead directly heated by the beams with a range adequately short as to stop within its thickness [22].

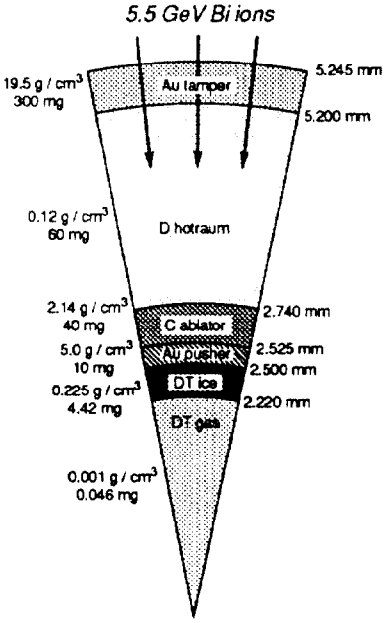

Fig. 7. *Diffuse geometry for ID pellet. From Basko [28].*

A preliminary design for such a pellet (Fig. 7) has been carried out by Basko [28]. Fusion is driven by a 7.5 MJ, 13 ns long, time modulated pulse of Bismuth ions. The gain, taking into account of the inefficiencies of ID, is about 80. The *hohl-raum* is filled with Deuterium in which ions stop ("hot-raum"). The relatively large size of the pellet (1 cm diameter) is adequate for low energy beams.

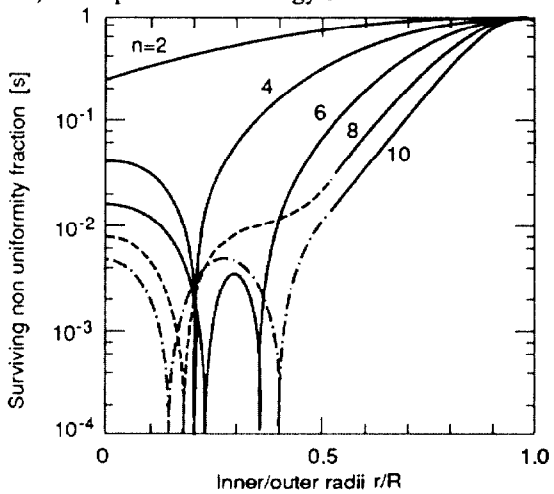

Fig. 8. *Smoothing effect of ID after first reflection [29].*

Such geometry permits a remarkable drive uniformity. This can be achieved in two steps:

(1)The transfer of the non-uniformities from the outer to the inner shells can be greatly reduced for the higher Legendre modes [29] with an appropriate ratio of the two radii (Fig. 8).

(2)As pointed out by Basko [28], the main surviving n=2 mode can be cancelled with a suitable beam configuration i.e. at a "magic angle" for the geometry of Fig. 9. Such a value is somewhat dependent on the geometrical profile of the beams from the driver.

The diffuse radiator solution has advantages both from the point of view of a practical realization of an "industrial grade" pellet and in order to minimize the requirements on the accelerator driver. Hence it is important that related calculations are vigorously pursued.

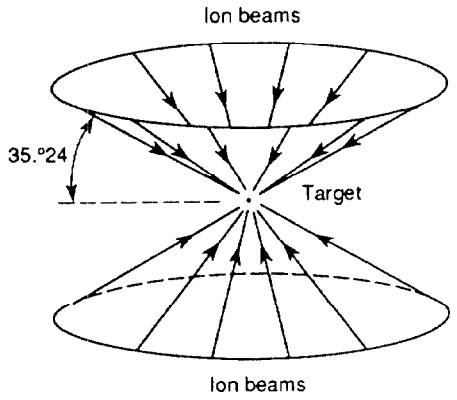

Fig. 9. *Optimized beam configuration to cancel the n=2 Legendre mode [28].*

5. THE ACCELERATOR COMPLEX.

5.1. General considerations. The accelerator complex must deliver some 5–10 MJ of energy in a time window of 10–15 ns. Its detailed design directly reflects the "state of the art" of the pellet design. For direct drive, nowadays less popular than in the past, the beam spot must have a radius of 4–5 mm. For indirectly driven targets and filamentary radiators it must be very small (≈ 1 mm radius) and ensure energy depositions of 10^{16}+ 10^{17} W/g on several (≥6) targets. Finally for a diffused radiator, while the spot size can be large (≈1 cm diameter), the energy of the beams must be considerably lower to ensure a short range, thus enhancing space charge effects in the beam transport and storage.

Although exotic focussing systems can be proposed, in the present paper we shall limit space charge considerations to those for "ballistic" and stable propagation in vacuum. To minimize space charge forces one must store ions stripped of as few of their electrons as possible. In our case the ion charge is set to q = 2, the lowest final charge state for which photo-ionization is working. The lifetime of such a beam is limited in practical cases to a few seconds because of inelastic intra-beam scattering which changes the charge states: $I^{(+2)}$ + $I^{(+2)} \Rightarrow I^{(+1)}$+ $I^{(+3)}$. Hence the whole manipulation time must be reduced to a few tens of milliseconds in order to keep beam losses to the few percent level.

A practical scheme [22] consists of a linear, single pass accelerator followed by a set of storage rings. A type of accelerator which would satisfy the efficiency requirements and of well-known performance is a conventional LINAC. Currents <i> in the range 50–100 mA for singly ionized heavy ions are possible. The energy E_{beam} transported by such a beam of kinetic energy eT in a time Δt is E_{beam} = Δt <i> T/e. For T=10 GeV, <i> = 0.1 A, $E_{beam} = 10^7$ J, we find Δt = 10 ms. Since the duration of the pulse on the pellet must be $\Delta\tau \approx 10$ ns, a compression factor of about $\Delta t/\Delta\tau \approx 10^6$ is needed. Such compression factors can be achieved with a set of storage rings and by having a large number of beams focussed simultaneously on the pellet. This last feature is also required to ensure uniformity of driving.

The most promising and simplest way of accumulating the required current in the rings is photo-ionization stacking [17], a method which introduces phase compression, thus eluding the conditions set by the Liouville theorem. With an intense U.V. light it is possible to ionize the beam from the LINAC from single to double thus storing it permanently in the ring(s). After storage there is no further effect of the U.V. light onto the beam as long as the energy of the photons is less than double to triple the ionization potential. After appropriate stacking and R.F. compression the several bunches of each of the beams are spliced into separate beamlets and transported to the combustion chamber.

Limitations due to space charge effects are crucial in defining the parameters of the scheme and they can be used to define a quite narrow feasibility window within the delineated general scenario. Out of the many different known types of instabilities which may plague a strong focussing storage and transport system, it turns out that the most relevant to our application are those associated to the transverse motion. In general, longitudinal effects can be controlled during the short duration of the storage [18]. One can consider three main critical areas :

(1) The first one is related to the high current stored in the beams of the storage rings during and particularly at the end of the stacking process. Limitations of this type usually occur in cyclic accelerators and they have been well studied at CERN and elsewhere.

(2) The second critical situation occurs at the last phase of bunch compression, just before beams are directed toward the pellet. Since relatively few turns in the rings and in the long beam transport are involved, the instabilities relevant here are those occurring in a single pass through a long beam transport section. There is a considerable amount of theoretical work and some experimental work on the subject. However our understanding of this regime is far less complete than in the case of cyclic accelerators.

(3) Finally, while throughout the beam transport beam-straws can be easily maintained shielded from each other, inside the reaction chamber they must converge in "free space". According to a first qualitative estimate, long-range forces between bunches near the final focus do not seem to be significant, at least as long as the spacing between straws is kept larger than a few

beam radii and the beam spot is large. In the case of filamentary radiators ($r \approx 1$ mm) the problem is no longer trivial and sophisticated correction devices may be required.

All the previous considerations apply to beams travelling in high vacuum. In the reaction chamber of a practical energy generating device operated at high rate, vacuum conditions are necessarily degraded by the previous explosions. The presence of (ionized) residual gas introduces new forces on the beam which must be studied.

Definition of the parameters of the complex can be best done backwards, namely setting first the condition resulting from the final beam transport and then adapting the storage rings and the LINAC characteristics to the requirements of the space charge limit to be reached in the final beam transport. These conditions can be reasonably met.

5.2. Space charge in the final transport. The high currents needed to implode the pellet produce a space charge defocussing which is comparable to the focussing forces of the beam transport channel. All sorts of instabilities may develop under such circumstances [19]. The phenomenon is even more complicated if external focussing — rather than being continuous, as in the case of solenoid focussing — is periodically modulated as in a FODO channel. Then in the presence of strong space charge forces, disruptive resonance effects are expected to occur for specific values of the combined focussing [20].

The maximum current through a beam transport section consisting of evenly spaced quadrupoles has been originally considered by Maschke [21] and further perfected by Hofmann et al. [20]. Experiments have shown that these limits are rather conservative. If one denotes with μ_0 the phase advance of betatron oscillation per focussing period in absence of space charge effects, standard theory in absence of the space charge effects ensures stability of particle motion for $\mu_0 \leq 180^0$. In the presence of strong space charge effects, one must require $\mu_0 \leq 90^0$ in order to avoid significant instabilities and even better maintain $\mu_0 \leq 60^0$ in order to avoid a pronounced instability of the third-order mode. If fourth and higher order instabilities must be avoided as well, the condition $\mu/\mu_0 > 0.4$ has to be imposed, where μ is the phase advance of betatron oscillation per focussing period in presence of space charge — i.e. for $\mu \geq 24^0$ if $\mu_0 = 60^0$.

The maximum number of ions per unit of length which can be transported in a FODO channel with a given μ is proportional to the emittance of the beam, related to the spot radius $\langle r \rangle$ and beam angular divergence $\langle \theta \rangle$ in the reactor chamber, $\varepsilon_{straw} = \langle r \rangle \langle \theta \rangle$. The beam angular divergence is in turn related to the solid angle (hence the area at the boundaries) occupied by the beam cross-section in the combustion chamber, $\Omega_{straw} = \pi \langle \theta \rangle^2$. In practice a large number of beams, denoted by S, will converge on the same target. The total solid angle subtended by the beams and for a given radiator is then $\Omega_{tot} = S\, \Omega_{straw}$. Since these openings let energy from the explosion escape in the form of radiation, they must be kept to a minimum and in general we shall consider Ω_{tot} as an input parameter. The size of the spot at the pellet determined by the physics of the pellet and the solid angle of the beam as subtended in the combustion chamber determine uniquely the beam emittance $\varepsilon_{straw} = \langle r \rangle / \sqrt{\Omega_{straw}\, \pi}$. As shown by Rubbia [22], the limitations of space charge in the final beam transport are characterized by the parameter Γ (dimensionally a length) related to the nature and the kinetic energy T of the ions, the space charge conditions and the required value of $E/\Delta\tau$:

$$\Gamma = \frac{4\pi r_o}{\beta^3 \gamma^3 c\ Q'\ K^{1/2}\ e\ T} \frac{E}{\Delta\tau} = a_o \left(\frac{E}{\Delta\tau}\right) \frac{1}{T^{5/2}}$$

$$r_o = \frac{q^2}{A} r_p \quad ; \quad a_o = \sqrt{2}\ \pi \frac{q^2 r_p m_p^{3/2} c^2}{Q'\ e} A^{1/2}$$

where q and A are relative to the ion beam, r_p and m_p refer to proton, $K = \pm B'/B\rho$ is the external focussing constant and $Q' \cong 1$ is tabulated in Ref. [20]. With $K = 0.267$ and $Q' = 1$, namely $\mu \geq 24^0$ and $\mu_0 = 60^0$ one finds (units in meters, Twatt and GeV) $a_0 = 1.181\ 10^{-2}$ for Barium and $a_0 = 1.449\ 10^{-2}$ for Bismuth (the choice of nuclei will be explained in paragraph 5.4). Once Γ is fixed, we can for instance set the values of Ω_{tot} and $\langle r \rangle$ and derive uniquely the main features of the beam(s) including the number of straws S and the parameters of the final focus :

$$\varepsilon_{straw} = \frac{\Gamma}{\pi S} = \frac{\Omega_{tot} \langle r \rangle^2}{\Gamma} \quad ; \quad \beta^* = \frac{\Gamma}{\Omega_{tot}} \quad ; \quad S = \frac{\Gamma^2}{\pi \Omega_{tot} \langle r \rangle^2}$$

Note that the emittance of each straw ε_{straw} is proportional to the peak power required $E/\Delta\tau$ and to the inverse of the number of straws which evidences the non-Liouvillian nature of the energy losses in the absorber. However, fixing Ω_{tot} causes the apparent paradox that the emittance for a fixed spot size varies as Γ^{-1}, namely inversely to the peak power $E/\Delta\tau$! Of course the number of straws S grows with the square of the peak power, $S \propto \Gamma^2 \propto (E/\Delta\tau.)^2$ in order to compensate for the variations of emittance. The beam optics inside the reactor chamber are totally determined by $\beta^* = \langle r \rangle / \langle \theta \rangle$, the beta function at the collision point, since $\beta(z) = \beta^* + z^2/\beta^*$ where z is the longitudinal coordinate (focal point at $z = 0$).

In the case of N identical focal points, each with S straw-beams focussed to the spot, the above relations hold also for the global Γ_{all} calculated for the total energy E_{all} on the pellet, the total number of straws N S and the correspondingly increased solid angle $\Omega_{all} = N\, \Omega_{tot}$:

$$\varepsilon_{straw} = \frac{\Omega_{all} \langle r \rangle^2}{\Gamma_{all}} \quad ; \quad \beta^* = \frac{\Gamma_{all}}{\Omega_{all}} \quad ; \quad N\,S = \frac{\Gamma_{all}^2}{\pi\, \Omega_{all} \langle r \rangle^2}$$

In Fig. 10 we display the relation between N S and the ion energy for a number of beam focal radii, having set the beam power and duration $E/\Delta\tau = 500$ TW and $\Omega_{all} = N\, \Omega_{tot} = 0.1$ sterad. Two possibilities emerge for a reasonable number of straws, $N\,S \approx 10^3$. In one case (B), the beam spots are focussed down to about 1–2 mm radius, corresponding to the "high-energy option" for beams of either Ba or Bi in the 9–10 GeV range. At this energy the range of ions is considerable and a relatively thick absorber is necessary. These are the appropriate conditions for filamentary radiators [11]. The second alternative (A) — more suited for the beam stopping in the ra-

diating shell of the *hohl-raum*— corresponds to a focal spot ≥ 5 mm radius and is implemented best with lower energy beams with the shortest range i.e. in the region 5–6 GeV.

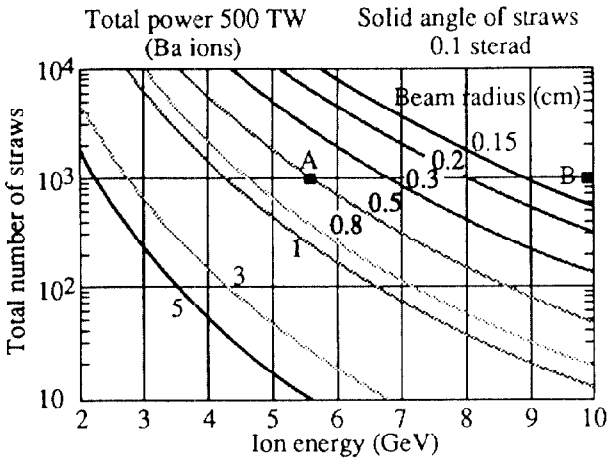

Fig. 10. *Limitations in the main parameters of the driver due to space charge effects in the final focus [22].*

The value of the beta function at the focal point, $\beta^*=\Gamma_{all}/\Omega_{all}$ is independent of the spot size, and is a function only of the main parameters $E/\Delta\tau \propto \Gamma_{all}$ and Ω_{all}. Experience with colliders has shown that values of $\beta^* \geq 5$ cm are possible with standard quadrupole focussing and beam parameters of the kind presently under consideration.

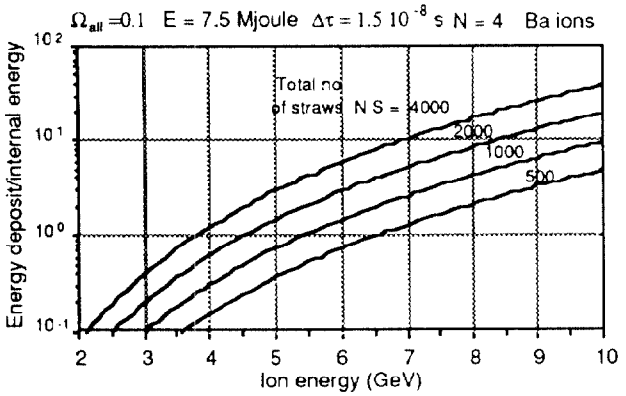

Fig. 11. *Specific energy Δ deposited by Ba beam in units of internal energy $\varepsilon_0(T_0)$ with T_0= 330 eV, N = 4.*

Another important parameter is the specific energy deposition Δ = E/V in the N targets averaged over its volume V ≈ $N\pi\langle r\rangle^2\rho(T)$, where ρ(T) is the range of ions (N = 4 corresponds also to a thin, spherical "diffused absorber"):

$$\Delta = \frac{E}{V} = \frac{S\,\Omega_{tot}\,\Delta\tau^2}{N\,a_0^2\,E}\,\frac{T^5}{\rho(T)}$$

Once N, E, Δτ, Ω_{tot} and S are chosen, $\Delta \propto T^5/\rho(T)$ exhibits the fast dependence on T, the beam energy. This energy deposition must be compared with the internal energy $\varepsilon_0(T_0)$ for a temperature T_0 (radiated and kinetic energies must be added). A simple parametrization [12] gives (T_0 in eV) :

Material	CH	Al	Au
ε_0(J/gram)	$4.0\ 10^4\ T_0^{1.2}$	$3.6\ 10^4\ T_0^{1.2}$	$2.2\ 10^3\ T_0^{1.6}$

Clearly this specific energy is so to speak "stored" in the absorber and in order to achieve an efficient implosion it must be substantially smaller than the delivered energy density i.e. $\varepsilon_0(T_0) \ll \Delta$. As apparent from Fig. 11, the kinetic energy of the beams is then the primary parameter, at least as long as ballistic beam transport in vacuum is considered. Note the generality of the condition which is independent of the geometrical parameters of the pellet.

5.3. Space charge in the Storage rings. Now that the parameters of the final focus have been narrowed down, we can consider the requirements on the storage rings which supply the ions. We shall neglect at this stage phase space blow-up and particle losses in these manipulations which consist simply of a longitudinal bunch compression followed by extraction and transfers. No bunch coalescence is used and therefore both the number of bunches and the total number of particles/bunch are conserved.

The total number of rings n_{rings} is related to the number of bunches h which can be stored in each ring, since S = $h \times n_{rings}$. The number of straws S, the beam transverse emittance ε and the number of ions in each straw N_{straw} are largely determined by the required properties of the final focus and the space charge limitations in the final transport section and are considered at this point as fixed. The total number of ions which can be stored in each ring, hence the number of straws (bunches) which can be constructed from each ring, is determined by the stability limit in the transverse plane due to the maximum incoherent tune shift (Laslett) at the much more "relaxed" bunching during storage and stacking :

$$N_{straw} = 4\,\pi\,\gamma^3\beta^2\varepsilon_{straw}\,\frac{1}{r_o}\,\frac{B}{h}\,\Delta Q \;;\; r_o = \frac{q^2}{A}\,r_p$$

where B is the bunching factor and ΔQ the largest allowed tune shift. One can relate this condition to the one of the final focus following Ref. [20] which can be rewritten as:

$$N_{straw} = \frac{1}{4\,r_o}\,\beta^2\gamma^3 K^{1/2}\,Q'\,\varepsilon_{straw}\,l_{straw}$$

where l_{straw} is the effective length of the beam straw at the pellet. Combining the two equations we find a simple expression giving the total straw length at the final focus that each ring can supply :

$$l_{straw}\,h = \frac{16\,\pi\,B}{K^{1/2}}\,\frac{\Delta Q}{Q'}$$

Note the purely "geometrical" nature of the expression above, which is independent of the nature, energy and transverse emittance of the ion beam. This is due to the fact that both limitations have a common physical origin.
Setting as values K = 0.25 m^{-2}, Q ≅ 1 , B = 1/2 and ΔQ ≅ 0.5, which is the largest value for the CERN-PS Booster [24], we find l_{straw} h = 25.12 m (note that $l_{straw} = \beta\,c\,\Delta\tau$ and for the typical values β = 0.3, Δτ = 10^{-8} giving l_{straw} = 0.9 m). These rather general considerations suggest that if h has to be the largest possible number of the form 2^k with k integer, then h ≅ 16 and therefore n_{rings} = S/h = S/16. Hence

the number of beam splittings which is optimal for the scheme is rather rigidly determined by space charge considerations.

5.4. Photo-ionization driven stacking. Stacking by photo-ionization can be induced along a straight section of the storage ring for the doubly ionized particles which we assume for simplicity to be a matched FODO quadrupole lattice. Injection occurs when the singly ionized beam from the LINAC collides head-on with an intense and monochromatic UV light beam. The most appropriate device to produce such a light appears to be a Free Electron Laser (FEL) [22]. Bending magnets at the beginning and the end are used to separate the orbit of the singly ionized beam of the LINAC from the equilibrium orbit of the stored beam since magnetic rigidities differ by a factor two. There is a difference in the parameters of the FODO channel between the singly and doubly charged beams and both beams must be separately matched outside the common straight section. If a parallel optical beam of uniform intensity is matched to the ion beam, the light power needed for an ionization efficiency η is

$$P_\gamma = -\log(1-\eta)\,\frac{\pi\ c\ (eV_\gamma)}{\sigma_{ion} n_{per}}\left(\frac{\varepsilon_0}{\pi}\right)\frac{1}{2\tan\frac{\mu^+}{2}\left(1+\sin\frac{\mu^+}{2}\right)}$$

where:

ε_0 is the invariant beam emittance,
c the speed of light,
e the elementary charge,
V_γ the photon energy in Volt,
σ_{ion} the peak photo ionization cross section,
n_{per} the number of FODO periods where collisions occur,

and μ^+ is the phase advance/period for the singly ionized ions in the channel, related to the phase advance μ^{++} for the doubly ionized ions for which the structure is tuned.

For Barium $\sigma_{ion} \approx 2\times10^{-15}$ cm^2 = 2×10^{-19} m^2, V_γ = 22 Volt, $\mu^{++} = 60^o$ we find $\mu^+ = 28.9^o$. Setting for the other parameters $n_{per} = 2$, $\eta = 0.90$ and $\varepsilon_0 = \pi\ 10^{-6}$ rad.m we find P_γ = 29.28 kW. Note that in the case of non-resonant ions (Ba) the light intensity required is considerably larger.

In the case of a matched light beam, P_γ is independent of the length of the periods. In principle a large number of periods can be used, with the ultimate limitation due to diffraction. Because of the difference in the betatron functions between singly and doubly ionized ions, emittance is not conserved through the ionization process even though the momentum transfer due to the ionization process is negligible. In practical conditions, a blow-up of some 20-30% has to be accounted for.

In the case of Barium, resonance peaks are very narrow (Fig. 12). This implies that both the photon energy and the ion speed must be defined with sufficient precision not to exceed the width of the resonance. While in the case of the FEL this appears as easily attainable and directly related to the stability of the electron energy, special care has to be exercised with the ion beam, since the Doppler effect shifts the photon energy in the laboratory. Peaks β and γ (see Fig. 12) have a width of 0.025 eV, sufficient to include a typical momentum spread $\Delta p/p = 10^{-3}$.

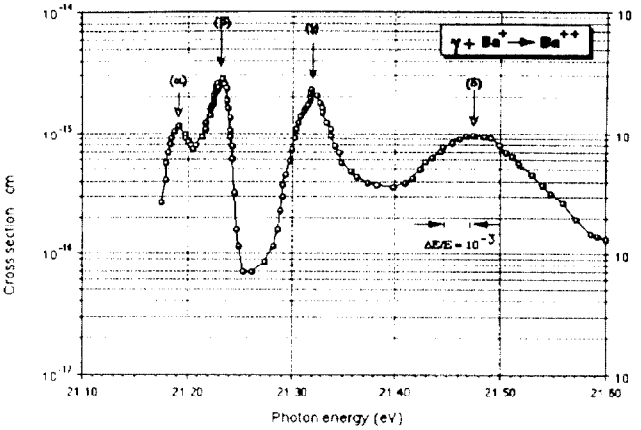

Fig. 12. *Ionization cross section for Ba^+ ions [27].*

The requirements on the light source indicate that the FEL must be driven by an electron LINAC. The general applicability of such a device to our case has been discussed in Ref. [22]. Subsequently it has been pointed out by Bonifacio et al. [25] that the required wavelength, namely $\lambda_{ion} \approx 80$ nm can be best produced with a two stage device in which light is first amplified at $3\lambda_{ion}$ followed by a triple, single-pass stage. This arrangement in particular allows an electron beam to be used whose properties are less stringent than those of a single pass stage. A fundamental condition for the operation of a FEL is related to the coherence of the source, which in turn can be expressed in terms of the emittance ε_{ele} of the electron beam, the so-called Pellegrini condition, $\varepsilon_{ele} \leq \lambda_{photon}$. Bonifacio et al. [25] have shown that with the help of a tripler stage this condition can be somewhat relaxed.

The first stage at 240 nm can be either an amplifier driven by an excimer Laser [25] or alternatively operated as an oscillator [26]. There are strong reasons in favour of the latter solution namely (1) difficulty of synchronizing an excimer Laser and the bunch structure of the LINAC, (2) existence of reasonably efficient mirrors for wavelengths in the region of 240 nm; (3) simplicity of the device since the electron bunch is driving the whole device. A very complete design for the Laser, to which we refer for details, has been given elsewhere [26]. One needs a peak bunch (B ≈ 0.1) current of about 200 A at 250 MeV with the invariant emittance of 1.7×10^{-5} rad.m which is within the state of the art of special photo-cathodes. Such a FEL will deliver 1 MW peak after 14.0 meters of undulator and will saturate at 69 MW after about 21 meters. Since the light power required by the photo-ionization is considerably smaller, one can reduce correspondingly the fraction of LINAC buckets which are filled. For instance, in order to produce an "average" power of 69 kW, largely sufficient for the case of Barium, the average LINAC current needs to be about 20 mA. The lasing efficiency of such a device is typically $\rho \approx 1.5 \times 10^{-3}$ and an energy recovery for the beam after the undulator is advisable.

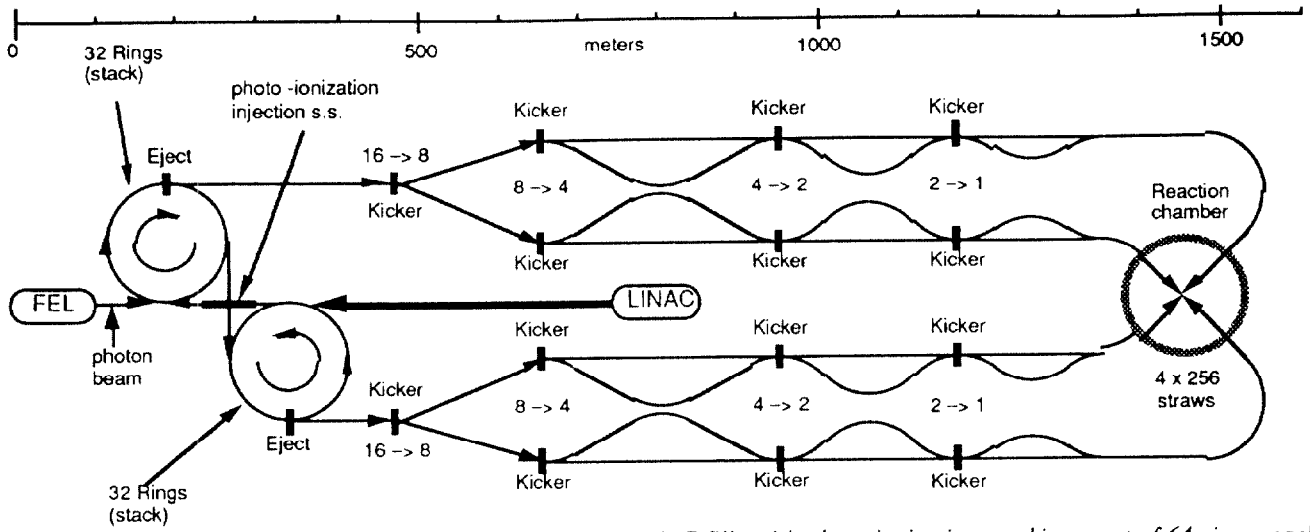

Fig. 13. *Schematic diagram of the driver from Ref [22]. A LINAC fills with photo-ionization stacking a set of 64 rings, each containing 16 bunches. Bunches in turn are split into separate, but isochronous 64 x 16 = 1024 beamlets with one bunch each which are directed onto the pellet. Photo-ionization is performed by a FEL, driven by an electron LINAC.*

5.5. A practical scheme. The general layout of the accelerator complex is shown in Fig.13. Parameters given in the Table are for four filamentary radiators heated by Barium beams at 10 GeV. For details we refer to Ref. [22].

The current of singly ionized ions from a LINAC can be typically of the order of 50-100 mA with an invariant emittance of about 1.0×10^{-6} π rad.m. Setting E =7.5 MJ, T = 10^{10} V, η = 0.9 and <i> = 50 mA where E is the total delivered energy, T is the ion kinetic energy in eV and η is the stacking efficiency. We find t_{fill} = 16.6 ms.

The beam from the LINAC is stacked in a relatively large number of storage rings (64). The optics of each ring is taken to be a simple FODO lattice with bending magnets inserted between quadrupoles. The storage time is close to the accumulation time during which the current is rising linearly in all rings as a function of time to the peak value which is of the order of a few amperes.

Table 2. Indicative values of lattice of rings and beam transport [22]

Type of lattice	FODO	
Nominal momentum p_o/q	31.4	GeV/c
Length of period, L	12.5	m
Free length between lenses	4.46	m
Length of lenses (magnetic)	0.90	m
Quadrupole gradient	20.00	Tesla/m
Phase advance, no space charge, μ_o	60	degr
Phase advance, full space charge, μ	24	degr
Beta functions @ $\mu = 60^o$ (no sp.ch.)		
-max, β_{max}	21.38	m
-min, β_{min}	7.28	m
Beta functions @ $\mu = 24^o$ (full sp.ch.)		
-max, β_{max}	32.13	m
-min, β_{min}	20.80	m
Admittance, true, α_{straw}	20.0π	μm*rad
Radial aperture ($\beta = \beta_{max}$; $\mu = 24^o$)	24.90	mm

There are constraints on the lattice coming from the necessity of transporting high currents during the last phase of accumulation. The optics of these rings (see Table 2) cannot be excessively sophisticated since the defocussing effects of the space charges introduce large detuning effects and major changes of the betatron functions during the stacking. Fortunately the momentum spread is relatively small and chromatic corrections can be neglected to a large extent.

For simplicity and in order to avoid matching problems in the presence of massive space charge effects, we assume that the whole complex from the injection in the ring to the final focus onto the pellet is a repetition of the same FODO lattice. Each ring is made of a FODO lattice with bending magnets inserted between equally spaced quadrupole lenses. Two periods in each of the four equally spaced super-periods are left empty for extraction, RF etc. As already pointed out there is need for a large number of such rings (64) to be filled in series from the LINAC and emptied in parallel toward the reaction chamber. The most reasonable geometry, following the example of the PS-Booster, is the one of a series of stacked rings, sharing the main elements of the magnetic structure. Since the number of rings is larger, the structure needs to be more compact and many rings (32) could be stacked vertically.

RF cavities are located in the long straight sections and are shared amongst all (or at least a group of) the rings of the stack. The RF is used to maintain the beam bunched during the stacking process with a relatively low bunching factor in order to be able to accumulate the largest possible number of ions around the circumference. Shortly before extraction the RF voltage is increased and appropriate RF manipulations allow the bunches to be compressed to the required length. This process must occur quickly enough not to cause beam losses due to crossing of betatron resonances. Extraction from all the rings is then performed simultaneously as a "one turn" extraction in one or several channels

and it requires a full aperture set of kickers with a rise time faster than the bunch spacing.

Separation of bunches is provided by an electrostatic deflector, which performs a transition half way during the passage of the beam in order to splice the bunch train. The two alternate paths are arranged in such a way as to bring into identical timing the two halves of the bunch train. With this technique one can separate out and synchronize 2^k bunches in k subsequent steps. The difference between the two paths, initially equal to half the circumference of the storage rings, is progressively reduced by powers of two at each step.

The final focus onto the pellet is the densest part of the beam straw geometry. The general layout is quite reminiscent of the low-β crossing in a high-energy collider. There is large latitude in the choice of the focal strength at the focus and the relatively modest momentum spread of the beams ($\Delta p/p \approx (1\text{–}2)\times 10^{-3}$) allows a modest effort in chromatic corrections. The range of ions in the absorber is very short (<< a few millimetres), there is in general little or no "focal depth" effect and full convergence on the pellet could be ensured even from large angles. The amount of radiant energy escaping the chamber is not negligible. It is therefore important that both the heat and the radiation are contained. Even 1% of the total energy may amount to as much as 10–20 Mwatt for a large scale power station. This can be achieved with the help of an s-shaped magnetic deflection and appropriate beam dumps. The possibility of using either pulsed lenses or permanent magnets should be examined.

6. CONCLUDING REMARKS.

A number of novel techniques developed in HEP may be beneficial to heavy ion induced confinement applications. Non-Liouvillian stacking appears feasible for Bismuth and very favourable for Barium. A bold extension of the multiple ring technique to ion stacking and ≈ 1000 beam straws would allow the design of rings with individual beams which remain in the domain of operation which has been well tested experimentally f.i. at CERN. Existing and proven techniques allow to reach parameters which meet likely conditions for indirectly driven ignition. These correspond to "high likelihood" cases for pellet implosion with high gain and directly relate to practical applications in the domain of energy generation.

7. ACKNOWLEDGEMENTS.

The author is very grateful to S. Atzeni, M.M. Basko, E. Bertolini, R. Bock, G. Dattoli, A. Hofmann, I. Hofmann, K. Hübner, J. Meyer-Ter-Vehn, D. Mohl, M. Puglisi, R. Ramis, P. Sievers, B. Zotter and A. Wrülich for participating in the elaboration of the concepts described in this paper.

8. REFERENCES.

[1] WEAVER T., ZIMMERMAN G. and WOOD L., *UCRL-74938* Preprint, October 30, 1973.

[2] NUCKOLLS J., LINDL J., THIESSEN A., WOOD L. and ZIMMERMAN G. *Nature* **239** (1972) 139 for the key idea. For excellent reviews DUDERSTADT J. and MOSES G.A., *Inertial Confinement Fusion* (New York: Wiley Interscience, 1982) or ARNOLD. R.C. and MEYER-TER-VEHN, J., *Rep. Prog. Phys.* **50** (1987) 559-606.

[3] LAWSON J., *Proc. Phys. Soc.* (London) **B70** (1957) 6.

[4] NAKAI S. et al. "In Laser Interactions and related phenomena" (to be published).

[5] ARNOLD. R.C. and MEYER-TER-VEHN J., *Rep. Prog. Phys.* **50** (1987) 559-606, for a comprehensive review .

[6] METZLER N. and MEYER-TER-VEHN J., *Laser Part, Beams* **2** (1984) 27.

[7] MEYER-TER-VEHN J. and SCHALK C., *Z. Naturf.* **37a** (1982) 955.

[8] BODNER S.E. *Phys. Rev. Lett.* **33** (1974) 761-4.

[9] TAYLOR G. *Proc. R. Soc.*, **A201**, (1950) 192-6.

[10] CHANDRASEKHAR S. *Hydrodynamic and Hydro magnetic Stability* (Oxford University Press, 1961).

[11] KULL H. *Phys. Rev.* **33** (1986) 1957 and refer. therein.

[12] WHITLOCK R. R. et al., *Phys. Rev. Lett.* **52** (1984) 819-22.

[13] SCHRIEVER R. L. et al., *J. Fusion Energy* **4** (1985) 116-8.

[14] MCCRORY, R.L.,VERDON, C.P., in *Inertial Confinement Fusion*, edited. by A. Caruso and E. Sindoni, (Compositori-SIF, Bologna, 1989), p. 183. ATZENI, S., *Europhys. Lett.* **11** (1990) 639; *Laser & Particle Beams*, in press (1991); *Particle Accelerators*, in press (1991).

[15] BASKO M.M. to be published in Nuclear Fusion.

[16] ATZENI S. private comm. and to be published.

[17] RUBBIA C. *Nuclear Instruments and Methods in Physics Research*, **A278** (1989) 253-265.

[18] HOFMANN I., *Proceedings of the 1984 INS-International Symposium on Heavy Ion accelerators and their Application to Inertial Fusion*, p 238.

[19] KAPICHINSKIJ I.M. and VLADIMIRSKIJ V.V., *Proc. 1959 Internat. Conf. High-energy Accelerators*, p 274 (CERN, 1959); DAVISON R.C. and KRALL N.A., *Phys. Fluids*, **13** (1970) 1543; GLUCKSTERN R.L. et al. *Proc. 1970 Natl. Accelerator Lab. Linear Accelerator Conf.*, **vol 2**, p. 823 (FNAL, 1970).

[20] HOFMANN I. et al., *Particle Accelerators* **13** (1983) 145-178.

[21] MASCHKE A.W., (1976), unpublished; REISER M., *Particle Accelerators* **8** (1978) 167.

[22] RUBBIA C. in *Proceedings of "Drivers for Inertial Confinement Fusion"* Osaka (1991) 74-96.

[23] MURAKAMI M., MEYER-TER-VHEN J. and RAMIS R. *Journ. of X-Ray Science and Technology* **2** (1990) 127-148.

[24] MOHL D., "Transverse space-charge effects in heavy ion storage ring(s) ", preliminary draft, CERN, Geneva (1991).

[25] BONIFACIO R., DE SALVO SOUZA L., PIERINI P. and SCHARLEMANN E.T. 1990 (unpublished).

[26] BARBINI R. et al., *ENEA Report*, RT/INN/90/35, ENEA, Frascati (1990).

[27] LYON L. et al. J. *Phys. B. At. Mol. Phys.* **196** (1988) 4737.

[28] BASKO M.M., private communication and to be published. I am indebted to Dr. Basko for having provided these preliminary data.

[29]MURAKAMI M., private communication and also CARUSO A.